10.1109/58.84297

Effect of Deep-Trap Level on Transverse Acoustoelectric Voltage Measurements

Fabrizio Palma, Giampiero de Cesare, Agostino Abbate, *Student Member, IEEE*, and Pankaj Das, *Member, IEEE*

***Abstract*—Transverse acoustoelectric voltage (TAV) measurements have been extensively used for the characterization of semiconductor properties. These measurements are rapidly becoming a powerful tool to study semiconductor processes and structures. The effect of trapped charges on the TAV is investigated in the present paper, with the aim of extending the use of TAV measurements to the study of semiconductors with high defect density. Even if SAW frequencies are as high as 100 MHz, charge trapping can influence the TAV. This has been verified by two particular experiments performed on Si/SiO_2 structures with high density of interface states. A theoretical model is proposed to explain the effects of the presence of deep-trap levels on the TAV. New boundary conditions for the acoustoelectric equations are introduced and an approximate solution for the TAV amplitude is presented. The model is used to define a new procedure for the determination of interface states' density using TAV versus bias voltage ($TAV - V_B$) measurements.**

I. Introduction

TRANSVERSE ACOUSTOELECTRIC VOLTAGE (TAV) measurements have been extensively used as a method for the characterization of semiconductor properties. Various techniques have been developed using TAV measurements, in order to determine a large number of semiconductor parameters. Measurements range from simple TAV versus bias voltage [1], [2], to one and two beam TAV spectroscopy [3], [4], temperature [5] and transient time measurements [6]. Using these techniques a large variety of materials have been characterized, among which Si and GaAs were the most extensively studied. Recently TAV measurements have been proposd as a tool for testing and studying complex structures, such as quantum layer substrates [4], [7] and high temperature ceramic superconductors [8]. A very interesting aspect of TAV techniques is the nondestructive nature of the measurements, which do not require any further technological process. This property ensures quick, *in situ* measurements and prevents from degradation of the characteristics of the sample under test.

Manuscript received March 16, 1990; revised February 6, 1991; accepted February 7, 1991. This work was supported in part by a NATO joint program with Grant No. 0750/87.

F. Palma and G. de Cesare are with the Universita Degli Studi Di Roma "La Sapienza," Dipartmento di Elettronica, Via Eudossiana 18, 000184 Rome, Italy.

P. K. Das and A. Abbate are with the Electrical, Computer, and Systems Engineering Department, Rensselaer Polytechnic Institute, Troy, NY 12180-3590.

IEEE Log Number 9101150.

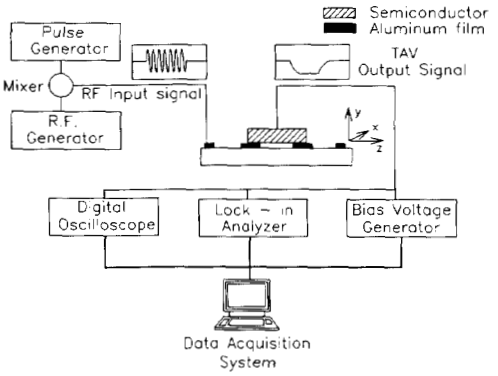

Fig. 1. Experimental setup for the TAV measurements using the separate medium structure.

The theory of TAV was developed after experimental results on Si/SiO_2 samples, i.e., a semiconductor structure which generally shows a low density of surface or interface states [9]–[12]. This theory at the moment needs to be updated in order to give correct interpretations of measurements performed on materials with a large number of bulk defects, such as amorphous semiconductors or semiconductors with a large number of surface states.

The schematic representation of the commonly utilized experimental arrangement is shown in Fig. 1. A small window, with 100 μm grating, is opened by photolithographic process on a thin aluminum film of approximatively 1 μm of thickness, deposited on the surface of the $LiNbO_3$ crystal. This window constitutes the interaction region. The semiconductor under test is placed on top of the crystal and pressed against the window. Interaction of the SAW rf electric field with the free carriers in the semiconductor gives rise to a dc acoustoelectric current. At open circuit conditions, the transverse acoustoelectric voltage (TAV) is detected at the back surface of the semiconductor.

The aluminum film also provides a ground path for the DC bias voltage that, applied to the semiconductor-insulator structure, changes the space charge density at the interface by field effect. Variation of the surface potential V_s due to the bias voltage V_B can be determined from TAV versus bias voltage ($TAV - V_B$) measurements by comparison and normalization with a theoretical expression of the TAV versus surface potential [1]. From this surface potential variation, the interface state density is inferred.

Various experimental results in the past years have pointed out the influence of deep-trap levels (DTLs) on

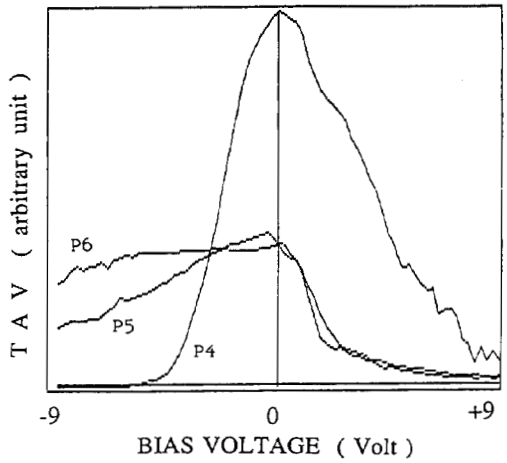

Fig. 2. $TAV - V_B$ measurements at two different SAW frequencies. Curve (a) corresponds to a f_{SAW} of 95 MHz, while curve (b) to 475 MHz. The Silicon sample is p-type, with 400 Å thermally grown silicon dioxide and high interface states' density.

TAV amplitude. Palma *et al.* [13] have shown that pressure-induced deep trap levels dramatically affected the TAV amplitude. In Fig. 2 three $TAV - V_B$ plots are shown; the curves were taken at different values of applied pressure. Comparison of curves shows that pressure produced an evident broadening of the $TAV - V_B$ curve and a drop of the maximum TAV voltage. Curve broadening provides an experimental evidence of the presence of surface traps at the Si–SiO_2 interface [14]. The generation of interface trap is thus associated with a sharp decrease in the TAV amplitude, pointing to a direct relationship between the amplitude of the TAV and trap density.

In order to determine the influence of DTL on TAV; a very interesting experiment was performed on p-type silicon samples with a 400-Å layer of thermally grown silicon dioxide and with a high density of interface traps [15]. The $TAV - V_B$ experimental plots shown in Fig. 3 were taken at two different SAW frequencies: 95 MHz, corresponding to the center frequency of the interdigital transducer, (curve *a*), and 475 MHz corresponding to the fifth harmonic of the transducer, (curve *b*). Between the two measurements only the RF SAW frequency was changed, ensuring an identical mechanical matching.

The different behavior of the $TAV - V_B$ plots at the two SAW frequencies can be explained by introducing the effect of the presence of interface trap levels into the theory of TAV. At the lower frequency, when the effect of DTL on TAV is relevant, a sharp quenching of the TAV amplitude is observed as the Fermi level, by means of the applied bias, approaches the trap level. At the higher SAW frequency the effect on TAV amplitude due to trap levels becomes less relevant and the quenching of the TAV is not observed. In this case, however, the Fermi level is pinned due to the presence of a large number of surface states.

The variation of the steady state trap population under the influence of the RF electric field was first presented by Moll, Otto, and Quate [16], and then suggested by

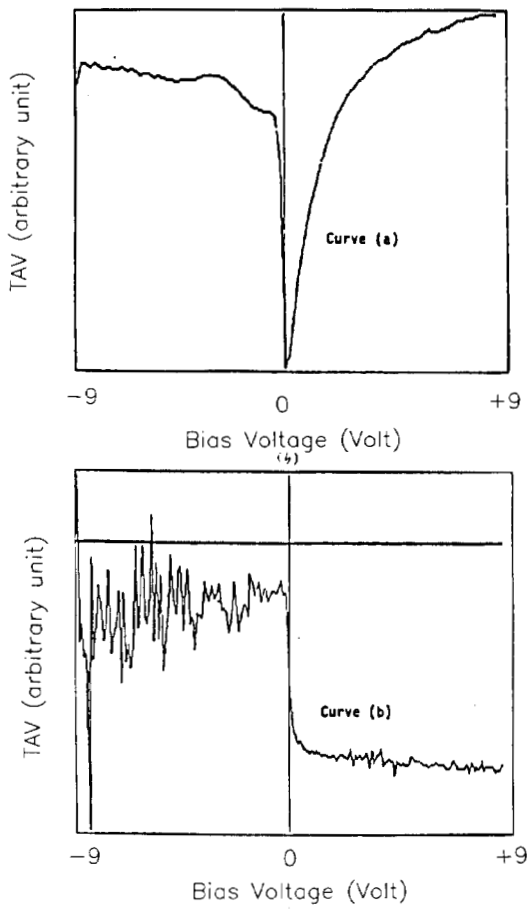

Fig. 3. Plot of the correction coefficient K_{it} versus SAW frequency with the net trap density N_t as a parameter. A single trap level is supposed to be located at the center of the bandgap, with capture coefficients $C_n = C_p = 10^{-9}$ cm^{3}s^{-1}. The silicon sample is assumed to be p-type with a carrier concentration of 10^{15} cm^{-3} and 10^{13} cm^{-3} for Fig. 4(a) and 4(b), respectively.

Fritz [11] as one of the mechanisms to be considered in order to correctly interpret TAV experimental results. Carriers are captured by traps during one half of the RF cycles and emitted from traps during the other half. Due to the nonlinearity of carrier modulation inherent in the acoustoelectric interaction these two processes have different rates, resulting in a net change in the trapped surface charge and in the generation of an additional current density term into the free carriers' equilibrium current equations. This current is very low, if compared to the total current of majority carriers, but it can dramatically affect the TAV amplitude, as only a very small and critical portion of the modulated charge gives rise to the nonlinear effect. Generally as a result of the trapping phenomena the TAV amplitude is quenched but extensive calculations and experimental results [17], [18] have shown that changes in the sign of TAV can occur.

The mathematical model of deep level kinetics is introduced in Section II and the new calculation of the theoretical TAV is discussed in Section III. Using this calculation, the procedure for the determination of interface states' density was modified, extending the use of TAV versus applied bias measurements to materials with high

defect density. This modification is outlined in Section IV and some experimental results are presented.

II. Mathematical Model of Recombination and Generation

Since the analysis of recombination and generation processes has been well established by Shockley and Read [19], we will briefly introduce it in conjunction with the practical model used in this study. The direct bandgap and Auger recombination processes as well as other generation processes such as photoexcitation are not considered in the following discussion.

The recombination and generation processes through a deep-trap level can be described by four transition processes: electron and hole emission, electron and hole capture [20], [21]. All these transitions are defined by emission or capture coefficients, respectively e_n, e_p (s^{-1}) and C_n, C_p ($cm^{-2}\ s^{-1}$). The net transition rates, i.e., the net change in the number of electrons (holes) per cm^2 s due to capture and emission, can be written as

$$R_n = -\frac{\partial n}{\partial t} = C_n p_t n - e_n n_t \tag{1}$$

$$R_p = -\frac{\partial p}{\partial t} = C_p n_t p - e_p p_t \tag{2}$$

in which $N_t = n_t + p_t$ is the net trap density/cm^2 at trap energy E_t, n_t is the number of trap levels/cm^2 that are filled with electrons and p_t the ones that are empty. Invoking the principle of detailed balance at thermal equilibrium, the carrier emission and capture processes are balanced [20], which yields to the following relationship:

$$e_n = C_n n_1 = C_n n_i \exp\left(\frac{E_t - E_i}{KT}\right) \tag{3}$$

$$e_p = C_p p_1 = C_p p_i \exp\left(\frac{E_i - E_t}{KT}\right) \tag{4}$$

where n_i and p_i are the intrinsic carrier concentrations and E_i is the intrinsic Fermi level; n_1 and p_1 are defined in (3) and (4) as the electron and hole concentrations calculated assuming that the Fermi level is positioned at the trap energy E_t. We want to emphasize that n_1 and p_1 are computable constants and not system parameters [20]. Note also that in the previous equations it is assumed that the semiconductor is not degenerate and that the trap level degeneracy factor is one.

Using (1)–(4), the net change in trap level occupancy can be calculated by

$$\frac{dn_t}{dt} = -\frac{\partial n}{\partial t} + \frac{\partial p}{\partial t} = R_n - R_p. \tag{5}$$

At thermal equilibrium, there is no net change in trap level occupancy; therefore we can calculate the equilibrium values of n_t and p_t, referred as n_{t_o} and p_{t_o}:

$$n_{t_o} = \frac{C_n n_o + C_p p_1}{C_n(n_o + n_1) + C_p(p_o + p_1)} N_t \tag{6}$$

$$p_{t_o} = N_t - n_{t_o} \tag{7}$$

where n_o and p_o are the equilibrium carrier concentration of the semiconductor.

Once the RF electric field of the SAW is applied, R_n and R_p differ from their equilibrium values and the relationship between the trap occupancy and recombination rates is given by

$$\frac{dn_t}{dt} = (C_n n + C_p p_1)N_t - [C_n(n_o + n_1) + C_p(p_o + p_1)]n_t. \tag{8}$$

Using a small signal approach and solving (8) we can thus calculate the small signal variation of the trapped charge, given by the different rates of capture and emission processes:

$$\Delta n_t = \frac{C_n p_{t_o} n' - C_p n_{t_o} p'}{j\omega + C_n(n_o + n_1) + C_p(p_o + p_1)} \tag{9}$$

where n' and p' are the small signal perturbations of the carrier concentrations, and $\omega = 2\pi f_{SAW}$ is the SAW angular frequency. The small signal recombination rates are defined, neglecting second-order terms, by the following relations:

$$r_n = C_n p_{t_o} n' - C_n(n_o + n_1)\,\Delta n_t \tag{10}$$

$$r_p = C_p n_{t_o} p' + C_p(p_o + p_1)\,\Delta n_t. \tag{11}$$

This is the generalized solution in which the recombination rate varies with the level of injection and it is a function of the perturbed carrier concentration and of the amount of band bending. Note that in both (10) and (11) the net recombination rates are given by the sum of two terms. The first term is frequency independent and represents the "classical" term of constant surface recombination velocity that is determined by the steady state space charge distribution of ionized levels. The second term takes into account the time dependence of the deep-trap levels space charge. At high SAW frequencies these second terms tend to zero but still their effects is important.

The aforementioned analysis was made for a single level interface trap, but surface centers are typically found to be continuously distributed in energy throughout the semiconductor bandgap. The net recombination rates associated with each single level must be added in order to obtain the overall recombination rate. The simple addition is possible because trap level at different energies are considered noninteracting, since inter-center transitions are extremely unlikely to happen [20].

The recombination–generation model discussed and presented above is incorporated into the acoustoelectric equations in order to determine DTL effects on the TAV. The procedure and results of computer simulation will be discussed in Section III.

III. Modified TAV Theory

In the present section new boundary conditions for the solution of TAV equations are introduced, taking into account the presence of deep-trap levels at the semiconductor-insulator interface. The semiconductor constitutive equation must be solved simultaneously for both carriers in the semiconductor [7], in order to calculate the TAV. This leads to a sixth order differential equation. The solution for the perturbation in the electric potential $\phi(y, z, t)$ consists of the sum of six terms given by

$$\phi(y, z, t) = e^{j(\omega t - kz)} \sum_{i=1}^{6} A_i e^{k\gamma_i y} \tag{12}$$

where k is the wave vector of the SAW, A_i are constants to be determined by appropriate boundary conditions, and γ_i are solutions of the characteristic equation of the system [10].

The new boundary conditions, taking into account the presence of DTL at the interface, are as follows.

1) Continuity of the electric potential at the interface.

2) Relation between the normal electric fields in the insulator and in the semiconductor at the interface ($y = 0$):

$$\epsilon_I E_I(0^-) = \epsilon_S E_S(0^+) - q\,\Delta n_t \tag{13}$$

where ϵ_I, ϵ_S are the dielectric constant for the insulator and the semiconductor, respectively.

3) Generation of small currents at the interface due to recombination-generation processes [20]:

$$J_n(0) = qr_n \tag{14}$$

$$J_p(0) = -qr_p. \tag{15}$$

Using these conditions, the electrical potential is calculated as following [7].

The TAV arises from the nonlinear interaction of the charge modulation and the RF electric field. The nonlinear current generates a stationary nonequilibrium distribution of charges, and the TAV is defined as the potential drop through the semiconductor. In order to show the effect of DTL on the TAV amplitude calculated by this analysis we will define two quantities: TAV_{it} and TAV_{th}, where the first is the updated expression for the acoustoelectric voltage and the second is the former theoretical expression calculated neglecting the effect of DTL [9]. The ratio between these two terms is represented by the factor K_{it} that is plotted versus the SAW frequency with the net trap density N_t as a parameter in Fig. 4. In this case we assumed the presence of a single deep trap level, located in the middle of the bandgap, with capture coefficients $C_n = C_p = 10^{-9}$ cm^3 s^{-1}. The silicon sample is assumed to be p-type with a carrier concentration of 10^{15} cm^{-3} in Fig. 4(a), and 10^{13} cm^{-3} in Fig. 4(b). The presence of a large attenuation for low values of SAW frequencies is evident. Fig. 4(b) also shows the possibility of change of sign of the TAV. This is due to the so-called "mixed modes," which arise above or in proximity to the dielectric relaxation frequency of the semiconductor. Because of the low concentration of majority carriers, the current generated by the trapping phenomena is more relevant and can produce phase mismatching between the current and the electric field and thus changes of sign of the TAV can occur.

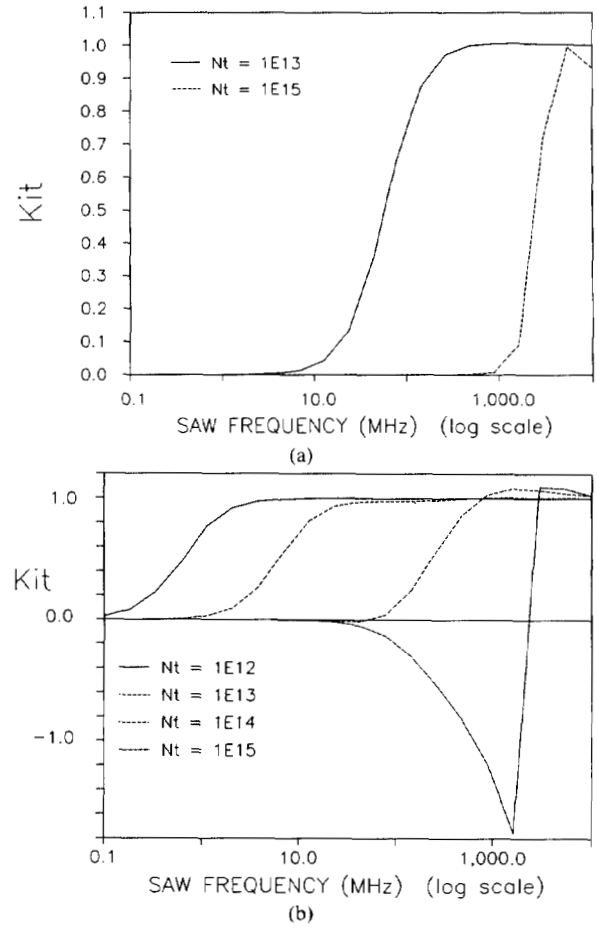

Fig. 4.

An approximate solution of the acoustoelectric equations is now introduced. The aim of this calculation is to obtain an explicit expression for the correction factor K_{it}, which multiplied to TAV_{th} will give us the updated value of the TAV amplitude, formerly defined as TAV_{it}. The correction factor K_{it} will be used for modifying the interface trap density measurement, as outlined in the next section. As pointed out before in Section II, at high values of SAW frequency, the term Δn_t in (9) drops to zero, therefore the small signal recombination rates can be approximated by

$$r_n = C_n p_{t_0} n' = S_n n' \tag{16}$$

$$r_p = C_p n_{t_0} p' = S_p p' \tag{17}$$

where S_n and S_p are the surface recombination velocities (cm/s) of electron and hole, respectively.

We can thus rewrite the boundary condition on the currents at the interface, as

$$J_n(0) = qS_n n' \tag{18}$$

$$J_p(0) = -qS_p p'. \tag{19}$$

The boundary condition of (13) becomes equivalent to

the continuity of the normal components of the electric displacement at the insulator–semiconductor interface.

Making the assumption that the semiconductor thickness is much larger than the penetration depth of the acoustoelectric interaction, we must set to zero the coefficients A_i of (12) with positive real part of γ_i. It can be shown [10] that only three solutions γ_i have negative real part. Moreover, for an extrinsic semiconductor, calculations [9] show that γ_3 is very close to unity and γ_1 is always one, while γ_2 can be considered a real quantity. Using this approximation we can impose $\gamma_1 = \gamma_3 = 1$ and $\gamma_2 = \gamma$ [9], and (9) becomes

$$\phi(y, z, t) = e^{j(\omega t - kz)}[A_1 e^{-ky} + A_2 e^{-\gamma ky}] \quad (20)$$

where the coefficients A_1 and A_2 are determined using the boundary conditions. Imposing (18) and (19), a relationship between the coefficients is established as

$$\frac{A_1}{A_2} = j\omega R_1 + k\left(S_n \frac{\omega_{DN}}{\omega^2} + S_p \frac{\omega_{DP}}{\omega^2}\right) = j\omega R_1 + R_2 \quad (21)$$

where

$$R_1 = \frac{\omega_{CN}^2 \omega_{DN} + \omega_{CP}^2 \omega_{DP}}{(\omega_{CN}\omega_{DN} + \omega_{CP}\omega_{DP})^2}\gamma \quad (22)$$

$$\omega_{CN} = \frac{q\mu_n n_o}{\epsilon_S}, \quad \omega_{CP} = \frac{q\mu_p n_o}{\epsilon_S} \quad (23)$$

$$\omega_{DN} = \frac{V_S^2}{D_n}, \quad \omega_{DP} = \frac{V_S^2}{D_p} \quad (24)$$

where μ_n, μ_p are the electron and hole mobility, respectively, D_n, D_p is the electron and hole diffusion coefficient, respectively, and V_S is the SAW velocity.

One can notice from (21) the effect of deep-trap levels. The ratio between the two amplitudes, formerly depending only on the first term on the right-hand side, now is modified due to the addition of a term related to the presence of trap levels. For a p-type silicon sample with a carrier concentration of 10^{15} cm^{-3} and with a single trap level located 0.4 eV below the conduction band, the ratio R_2/R_1 is 2×10^3 for a trap density $N_t = 10^{12}$ cm^{-2} and increases as N_t increases. In this example we have assumed $C_n = C_p = 10^{-9}$ cm^{3}s^{-1}.

From the boundary condition on the surface potential, the amplitude A_2 is determined to be

$$A_2 A_2^* = \frac{|\phi_o|^2}{|1 + j\omega R_1 + R_2|^2} \quad (25)$$

where ϕ_o = SAW RF potential at the surface of the piezoelectric material.

We can thus obtain an explicit expression for the correction coefficient K_{it} to be multiplied to the former theoretical expression TAV_{th} present in literature, in order to obtain the updated expression for the TAV, TAV_{it}.

$$K_{it} = \frac{TAV_{it}}{TAV_{th}} = \frac{(1 + \omega^2 R_1^2)}{|1 + j\omega R_1 + R_2|^2} \quad (26)$$

The correction factor K_{it} calculated using (26), is plotted versus the SAW frequency in Fig. 5, where the semiconductor is a p-type silicon with 10^{15} cm^{-3} carrier concentration. The curves are plotted with N_t as a parameter and

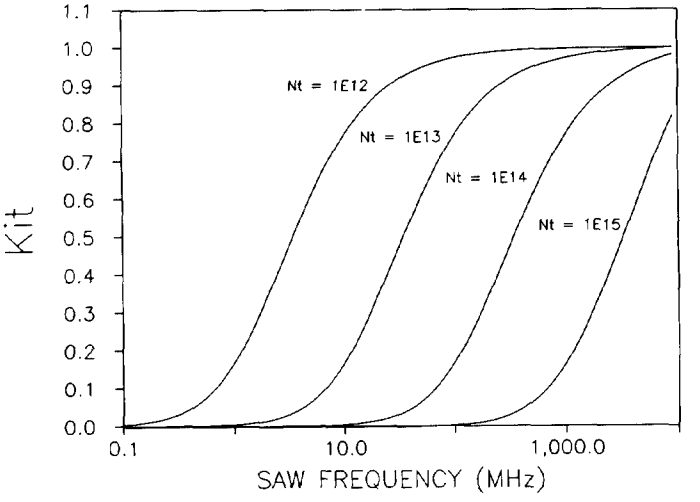

Fig. 5. Plot of the correction coefficient K_{it} versus SAW frequency. The silicon sample is assumed to be p-type with a carrier concentration of 10^{15} cm^{-3}. Silicon sample P = 1E15, $C_n = C_p$ = 1E − 9.

$C_n = C_p = 10^{-9}$ cm^{3}s^{-1}. A single trap level is assumed to be located 0.4 eV below the conduction band edge. TAV quenching at lower frequencies as a function of the number of trap levels can be seen. In the range of frequency commonly used for TAV measurements (55–100 MHz) the approximation is in good agreement with the complete and more exact numerical solution. This approximate solution can be assumed to be valid as long as the SAW frequency is lower than the dielectric relaxation frequency of the semiconductor.

IV. New Interface Trap Density Measurement

As already mentioned, the density of trap levels D_{it} at a semiconductor surface or interface can be determined using TAV measurements. The principle of this measurement is very similar to the widely used C–V technique. Variations of the surface potential V_S due to the applied bias voltage V_B can be determined from TAV versus bias voltage measurements $TAV - V_B$ by comparison and normalization with the theoretical expression of the TAV versus surface potential $TAV - V_S$. The difference between the two curves is attributed to the stretchout effect caused by interface states. The interface trap density D_{it} is therefore calculated [1] as

$$D_{it} = \frac{C_{TA}}{q}\left[\left(\frac{dV_S}{dV_B}\right)^{-1} - 1\right] - \frac{C_D}{q} \quad (27)$$

where C_{TA} is the coupling capacitance [13] and C_D is the space charge capacitance per unit area [22].

The block diagram of the D_{it} calculation is shown in Fig. 6. The acquisition of the experimental data is performed by an IBM-PC computer as shown in Fig. 1, and by an appropriate program the density of interface states is calculated. Results obtained with this technique are in good agreement with other measurements. In view of the theory outlined in this paper, the TAV is a function of the surface trap density; therefore the $TAV - V_S$ plot must also change with different trap densities. In Fig. 7 the TAV_{it} amplitude is plotted versus the surface potential V_S, with the net trap density N_t as a parameter. A single trap

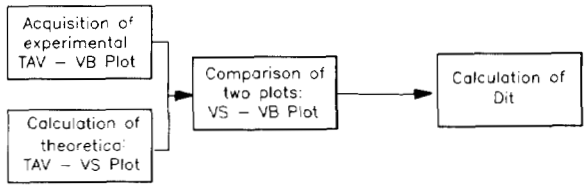

Fig. 6. Block diagram of the density of trap levels calculation procedure using $TAV - V_B$ measurements.

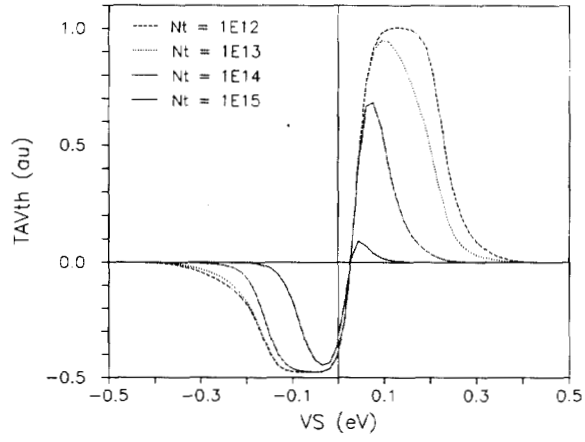

Fig. 7. TAV versus surface potential theoretical $TAV_{it} - V_S$ curve plotted as a function of the net trap density N_t. A single trap level is assumed to be located in the middle of the bandgap with $C_n = C_p = 10^{-9}$ cm^{3}s^{-1}.

level is assumed to be located in the middle of the bandgap with $C_n = C_p = 10^{-9}$ cm^{3}s^{-1}. As shown, the shape of the $TAV - V_S$ plot changes dramatically as the trap density increases. Note that the net trap density must be above 10^{13} cm^{-2} in order to have a sharp variation of the $TAV_{it} - V_S$ curve from the $TAV_{th} - V_S$ plot.

In order to obtain a more accurate determination of the density of trap levels the new $TAV_{it} - V_S$ curve must be used. Since to calculate TAV_{it}, by means of (26), the density of surface trap levels must be known; a feedback loop in the D_{it} calculation is needed. A new measurement procedure is thus defined, and its block diagram is shown in Fig. 8. As a starting point the correction coefficient is set to one for all values of surface potential, and afterwards is calculated by means of the theory outlined in the previous section. After few iterations, successive D_{it} plots converge to what is believed to be a more accurate determination of the interface states' density.

The D_{it} measurements were performed on Si–SiO_2 samples, and results from the previous and new procedures where compared. For low interface states density Si–SiO_2 samles, the difference in results obtained with the two procedures is negligible, as shown in Fig. 9. In Fig. 9 the interface trap density is plotted as a function of the trap energy relative to the valence band edge, $E_{it} - E_v$ (eV). As we would expect for this sample the difference is negligible as the DTL density is very low and the correction coefficient is almost one for all values of V_S. On the other hand, results from measurements performed on a damaged Si–SiO_2 structure with a large density DTL, are not the same for the two calculation procedures. In this case the influence of DTL on the TAV amplitude cannot be neglected, and a shift of the position of the deep trap level

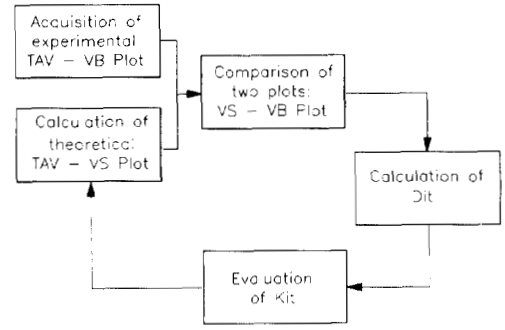

Fig. 8. Block diagram of the modified density of trap levels calculation procedure using $TAV - V_B$ measurements which takes into account the effect of DTL on TAV.

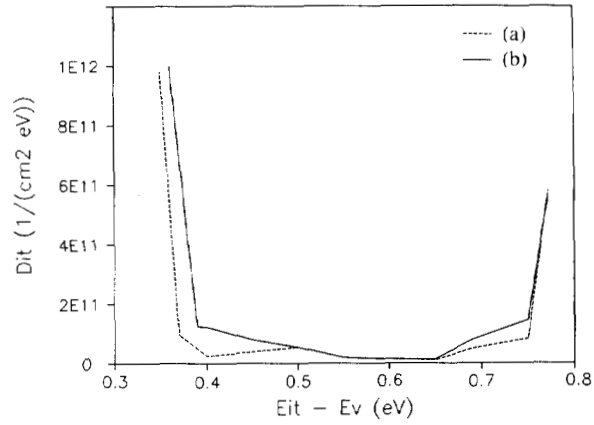

Fig. 9. $E_{it} - E$ curve for a Si–SiO_2 sample. Curve (a) was obtained using the previous procedure while curve (b) was obtained using the modified procedure.

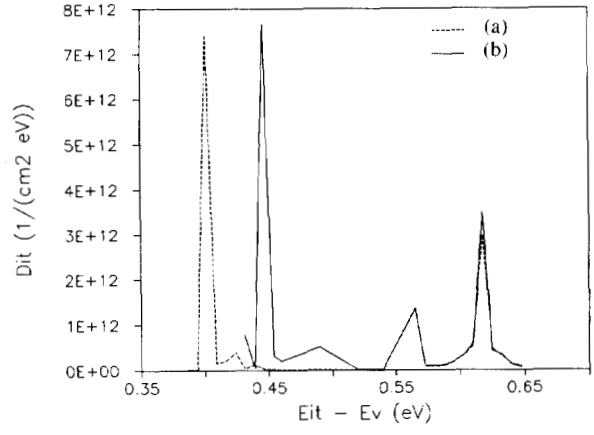

Fig. 10. $D_{it} - E$ curve for a damaged Si–SiO_2 sample. Curve (a) was obtained using the previous procedure while curve (b) was obtained using the modified procedure.

is obtained using the more accurate computation. The error in the determination of the position in energy of the DTL is 45 meV, a value comparable with the resolution of C–V measurements. A larger difference is obtained for measurements performed on compound semiconductors or materials with a larger number of surface defects. In this case large errors can occur if the old TAV measurement procedure is utilized, and an increase in time of computation is expected. Further improvements need to be made in order to achieve a better resolution for D_{it} calculations with TAV measurements with these materials.

V. Conclusion

The need of considering the effect of deep trap levels in TAV theoretical calculations was demonstrated by two particular experiments. As a result the presence of deep trap levels had to be considered for correct interpretation of any experimental result involving TAV measurements. A model for describing DTL kinetics was presented, along with new boundary conditions to be used in the characteristic acoustoelectric equations for calculating the transverse acoustoelectric voltage. In order to develop a new procedure for determination of interface states' density, an approximate solution for the TAV was presented, introducing a correction factor that describes the effect of DTL. The new D_{it} measurement procedure was tested on Si–SiO_2 structures, showing no difference in results for low interface trap density samples. But as the number of trap levels increases a change of the theoretical $TAV - V_S$ curve occurs, as a consequence a shift in the energy position of the measured level is observed.

References

[1] B. Davari, M. Tabib-Azar, T. Liu, and P. Das, "Nondestructive evaluation of the semiconductor interface states' density using the transverse acoustoelectric voltage," *Solid State Electron.*, vol. 29, no. 2, pp. 75–81, 1986.

[2] B. Davari, P. Das, and R. Bharat, "Semiconductor surface characterization using transverse acoustoelectric voltage versus voltage measurements," *J. Appl. Phys.*, vol. 54, no. 1, pp. 415–420, 1983.

[3] B. Davari and P. Das, "A study of the high resistivity GaAs surface and the GaAS/oxide interface using two-beam transverse acoustoelectric voltage spectroscopy," *J. Appl. Phys.*, vol. 53, ppp. 3668–3671, 1982.

[4] M. N. Abedin, P. Das, and F. Palma, "Study of electronic levels in a $GaAs/Al_xGa_{1-x}As$ single quantum well using surface acoustic wave technique," *Superlattice and Microstructures*, vol. 6, no. 1, pp. 7–11, 1989.

[5] M. Tabib-Azar and P. Das, "Surface Acoustic Wave-superlattice interaction in separate-medium structure," *Superlattices and Microstructures*, vol. 4, no. 4, pp. 643–651, 1988.

[6] M. Tabib-Azar and F. Hajjar, "Deep level transient spectroscopy of $Al_xGA_{1-x}As/GaAs$ using nondestructive acoustic-electric voltage measurements," *IEEE Trans. Electron Dev.*, vol. ED-36, pp. 1189–1196, 1989.

[7] F. Palma and P. Das, "Acoustoelectric Interaction in layered semiconductor," *IEEE Trans. Ultrason. Ferroelect. Freq. Contr.*, vol. UFFC-34, pp. 376–381, 1987.

[8] M. N. Abedin, S. C. Tiersen and P. Das, "Acoustoelectric effects in ceramic high-temperature superconductors using separate medium structure," *Appl. Phys. Lett.*, vol. 54, no. 26, pp. 2725–2727, 1989.

[9] P. Das, M. K. Roy, R. T. Webster, and K. Varahramyan, "Nondestructive Evaluation of Si wafers using SAW," IEEE Pub. No. 79Ch 1482-9, 1979, pp. 278–283.

[10] H. Gilboa and P. Das, "Nondestructive evaluation of electrical properties of semiconductors using SAW," ONR Tech. Rep. MAONR-15, 1977.

[11] I. J. Fritz, "Transverse acoustoelectric effect in the separated-medium surface-wave configuration," *J. Appl. Phys.*, vol. 66, no. 11, pp. 6749–6756, 1981.

[12] F. Palma, "A new theoretical model for transverse acoustoelectric voltage measurements on Si/SiO_2 structures," *J. Appl. Phys.*, vol. 66, no. 1, pp. 292–298, 1989.

[13] F. Palma, A Abbate and G. de Cesare, "New measurement structure for TAV testing of semiconductor: An experimental analysis," in *Proc. IEEE Ultrason. Symp.*, 1988, pp. 223–227.

[14] A. Abbate and F. Palma, "Study of Si/SiO_2 interface by transverse acoustoelectric voltage measurement," *Appl. Phys. Lett.*, vol. 55, no. 13, pp. 1306–1308, 1989.

[15] F. Palma, G. de Cesare, A. Abbate, and P. Das, "Effect of SAW frequency on transverse acoustoelectric voltage measurements," *Proc. IEEE Ultrason. Symp.*, 1989, pp. 117–121.

[16] N. J. Moll, O. W. Otto, and C. F. Quate, "Scanning optical patterns with acoustic surface waves," *J. Physique*, suppl. C6 au nos. 11–12, tome 33, pp. 231–234, 1972.

[17] H. Gilboa and P. Das, "Transverse acoustoelectric voltage inversion and its application to semiconductor surface study: CdS," *Surf. Sci.*, vol. 62, pp. 536–540, 1977.

[18] H. Estrada-Vasquez, R. T. Webster, and P. Das, "Transverse acoustoelectric voltage (TAV) spectroscopy OH high resistivity GaAs," *J. Appl. Phys.*, vol. 50, no. 7, pp. 4942–4950, 1979.

[19] W. Schokley and W. T. Read, "Statistic of the Recombination of holes and electron," *Phys. Rev.*, vol. 87, pp. 835–842, 1952.

[20] R. F. Perriet, *Advanced Semiconductor Fundamentals*. New York: Addison-Wesley, 1987, pp. 160–170.

[21] A. Chiabrera, "Semiconductors' characterization: kinetics of one energy-level recombination centers and surface states," *Solid State Electron.*, vol. 15, pp. 277–284, 1972.

[22] R. H. Kingston and S. F. Neustadter, "Calculation of the space charge, electric field and free carrier concentration at the surface of a semiconductor," *J. Appl. Phys.*, vol. 26, no. 6, pp. 718–720, 1955.

Fabrizio Palma was born in Rome, Italy, on October 18, 1954. He received the "Laurea in Ingegneria Elettronica" from the University "La Sapienza," Rome, Italy. He is a professor in the Electronics Department of the Rome University "La Sapienza," Rome, Italy. He has been working for several years on surface acoustic wave and acousto-optic interaction. He is now involved with semiconductor testing and amorphous semiconductor.

Giampiero de Cesare was born in Rome, Italy on October 13, 1954. He received the "Laurea in Ingegneria Elettronica" from the University "La Sapienza," Rome, Italy.

He is a Researcher in the Electronics Department of the Rome University "La Sapienza," Rome, Italy. He has worked on microelectronics technologies and liquid crystal and is now involved with semiconductor testing and amorphous semiconductor.

Agostino Abbate (S'86) was born in Fondi, Italy in July 1963. He received the "Laurea in Ingegneria Elettronica" from the University "La Sapienza," Rome, Italy. He is presently working toward the Ph.D. degree in the Electrical, Computer and System Engineering Department at Rensselaer Polytechnic Institute, Troy, NY. His current research interests include acousto-electric interaction in semiconductor and semiconductor testing.

Mr. Abbate is a member of the IEEE Electron Device Society and Sigma Xi.

Pankaj K. Das (M'66) received the B.Sc., the M.S., and Ph.D. degrees in electrical engineering in 1957, 1960, and 1964, respectively, from the University of Calcutta, Calcutta, India.

He is a Professor in the Electrical, Computer and System Engineering Department at Rensselaer Polytechnic Institute, Troy NY. He was formerly a Faculty Member with the Electrical Engineering Department of the Polytechnic Institute of New York and the University of Rochester. He has published numerous papers and is currently performing research in CCD and SAW signal processing devices, acoustooptics, and nondestructive testing using ultrasonic waves.